THE JOURNAL OF PHYSICAL CHEMISTRY A

Article

pubs.acs.org/JPCA

Velocity Map Imaging Study of the Reaction Dynamics of the H + CH_4 → H_2 + CH_3 Reaction: The Isotope Effects

Huilin Pan,[†] Jiayue Yang,[†] Quan Shuai,[†] Dong Zhang,[†] Weiqing Zhang,[†,‡] Guorong Wu,*[,†,‡] Dongxu Dai,[†,‡] Bo Jiang,[†] Donghui Zhang,[†,‡] and Xueming Yang*[,†,‡]

[†]State Key Laboratory of Molecular Reaction Dynamics, Dalian Institute of Chemical Physics, Chinese Academy of Sciences, Dalian, Liaoning 116023, China

[‡]Synergetic Innovation Center of Quantum Information & Quantum Physics, University of Science and Technology of China, Hefei, Anhui 230026, China

ABSTRACT: Following our previous study on the H + CD_4 → HD + CD_3 reaction [*Proc. Natl. Acad. Sci. U.S.A.* **2010**, *107*, 12782], the reaction of H + CH_4 → H_2 + CH_3 at collision energies ranging from 0.72 to 1.99 eV is studied using crossed-beam and time-sliced velocity map ion imaging techniques. The product angular and translational energy distributions at four different collision energies were derived from the measured images. The excitation function was also measured from these images together with a careful calibration of the H atom beam intensities at different collision energies. All of these results are compared with those of the H + CD_4 reaction to investigate the isotope effects. The isotope effects are all observed in the product angular distributions, the translational energy distributions, and the excitation function and further confirm the reaction mechanism proposed in the previous study on the H + CD_4 reaction.

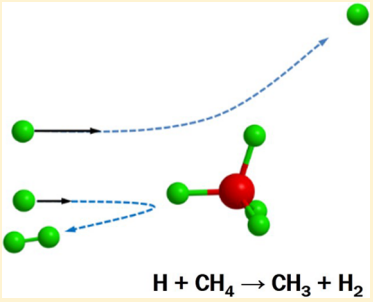

1. INTRODUCTION

The H + CH_4 → H_2 + CH_3 reaction is a prototype of polyatomic reactions, and understanding of this reaction has great implications in organic chemistry, combustion, interstellar chemistry, and fundamental reaction dynamics. It has attracted intense studies from both experimental[1−8] and theoretical[5−16] fields. Experimental studies have focused on both kinetics and dynamics of this reaction and the reverse. Theoretical efforts have been mainly devoted to potential energy surface (PES) construction and dynamical calculations. Understanding of the title reaction has been greatly improved through the interplay between the experiments and theoretical calculations.

In 2010, we performed a very detailed study on the H + CD_4 reaction in an extended collision energy region by combining the state-of-art crossed-beam scattering experiments and high-level quantum dynamical calculations.[8] Excellent agreements were achieved between experiments and theory, improving the understanding of reaction dynamics of the title reaction. At collision energies just above the barrier height, the integral cross section (ICS) rapidly increases with the increase of collision energy. When the collision energy is far above the barrier height, the ICS declines with the further increase of the collision energy. At the collision energies studied, the CD_3 products are predominantly backward/sideways scattered in the center-of-mass frame relative to the incident CD_4 beam. However, when the collision energy is far above the energy barrier, the backward scattered CD_3 products start to decrease. A reaction mechanism was proposed; all reactive events occur through a tug-of-war between the incoming H atom and the nonreacting CD_3 group. Above the threshold, collisions with large impact parameters start to contribute, causing a rapid increase of ICS. However, at collision energies far above the energy barrier, the incoming H atom moves too fast to be caught up by the slow D atom, causing a depression of reactivity, especially for collisions with small impact parameters.

In this article, we report our continuing experimental study on the H + CH_4 → H_2 + CH_3 reaction at collision energies of 0.72, 1.06, 1.66, and 1.99 eV. The experimental results are compared with those of the H + CD_4 → HD + CD_3 reaction extensively in order to investigate the isotope effects.[8] This study on the H + CH_4 → H_2 + CH_3 reaction further verifies the mechanism proposed previously. The remainder of the paper is organized as follows: The experimental details are described in section 2. In section 3, experimental results are presented and discussed. Conclusions will then follow in section 4.

2. EXPERIMENTAL METHODS

The experiment was carried out in a very similar way as our previous H + CD_4 experiment,[8] with the crossed-beam apparatus detailed previously,[17] combining time-sliced velocity map ion imaging and resonance-enhanced multiphoton ionization (REMPI) detection techniques. Briefly, the H atom beam was produced by photodissociation of HI molecules in a molecular beam. The HI beam was perpendicular to the reaction plane and intersected with a laser beam propagating in the reaction beam. After supersonic expansion at a backing pressure of about 1 atm, the parent HI molecules were dissociated to generate the H and I atoms. A small portion of

Received: February 17, 2014
Revised: March 15, 2014
Published: March 17, 2014

   dx.doi.org/10.1021/jp501681h | *J. Phys. Chem. A* 2014, 118, 2426−2430

the nascent H atom products traveling in the reaction plane entered the reaction/detection chamber through a skimmer (Beam Dynamics, Model 1). This selected portion of H products forms a pure H atom source with a well-defined velocity determined by the wavelength of dissociation light. Laser beams of 248 nm from an excimer laser (Lambda Physik LPF 202I) and 266 nm from the fourth harmonic generation of the output of a Nd3+:yttrium aluminum garnet (YAG) laser (Continuum, Powerlite Precision II 8000) were used. This produces a H beam with four different velocities due to the two spin−orbit iodine channels for the HI photodissociation at each dissociation wavelength.[18] The methane beam was generated by supersonically expanding neat CH_4 sample at a backing pressure of 4 atm from a pulsed valve (General Valve). The CH_4 beam also entered the reaction/detection chamber through a skimmer (Beam Dynamics, Model 1) and crossed with the H atom beam at an angle of 140°. From this, we obtained four collision energies of 0.72, 1.06, 1.66, and 1.99 eV. The difficulty of the experiment was to suppress the background as much as possible due to the very small reaction cross section.[3] The entire passage of the dissociation laser through the reaction/detection chamber was shielded by a tube in order to prevent the background caused by stray light.

The nascent CH_3 products were state-selectively detected by a (2 + 1) REMPI scheme via the intermediate $3p_z\,^2A_2''$ state.[19] The detection laser beam at around 330 nm (5−6 mJ/pulse) was produced by frequency doubling the output of a dye laser (Sirah PrecisionScan) pumped by a YAG laser (Continuum, Powerlite Precision II 8000). The CH_3 ions were projected onto an image-quality microchannel plate (MCP, BURLE Industries, Inc.) detector and recorded with a charge-coupled device (CCD) camera. Only images of ground vibrational state CH_3 products were recorded by tuning the laser wavelength at the peak of the Q-branch of the 0_0^0 transition. The CH_3 products with one quantum excitation in the umbrella mode (ν_2 = 1) were found in REMPI spectra measurements in previous experiments, but with a much smaller signal.[20]

3. RESULTS AND DISCUSSION

Images of the $CH_3(\nu = 0)$ products from the title reaction at the collision energies of 0.72, 1.06, 1.66, and 1.99 eV were recorded by fixing the laser wavelength at the peak of the Q-branch of the 0_0^0 transition, as shown in Figure 1a−d. All images are dominated by a single ring structure. A shift of the angular distributions from the backward at lower collision energies to sideways at higher collision energies is apparent. The rings become broader and more diffuse with the increase of the collision energy, indicating that the rovibrational excitation of the H_2 coproducts become hotter with the increase of the collision energy. Detailed angular and kinetic energy distributions were extracted from these images, after density-to-flux correction,[17,21] and will be discussed in the following sections. The excitation function was also measured by carefully calibrating the relative intensities of the H beam.

A. Angular Distributions. The product angular distributions were derived by integrating the corrected images along the radial directions, as shown in Figure 2a. The scattering angle is defined relative to the direction of the incident CH_4 beam in the center-of-mass frame. At all collision energies, the CH_3 products are backward/sideways scattered. The collision energy dependence of the products' angular distribution is very clear; with the increase of collision energy, the CH_3 products move from the backward direction forward toward the sideways

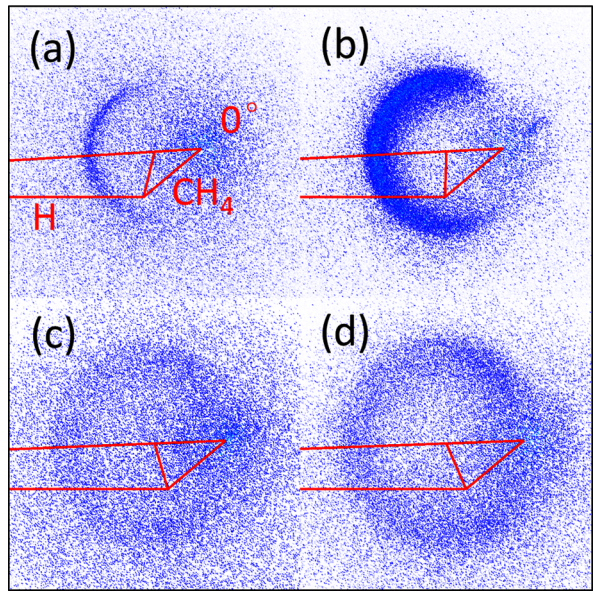

Figure 1. Raw images of the CH_3 products from the H + CH_4 → H_2 + CH_3 reaction at collision energies of 0.72 (a), 1.06 (b), 1.66 (c), and 1.99 eV (d), after background subtraction. The direction of the incident CH_4 beam in the center-of-mass frame is defined as the forward direction, as denoted in the figure.

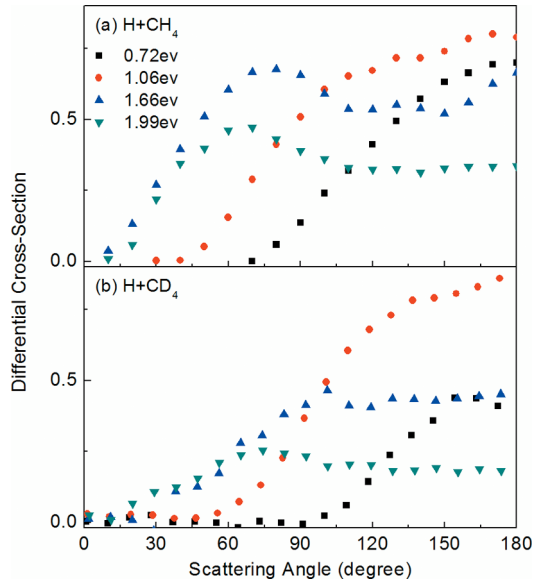

Figure 2. (a) Angular distributions of the CH_3 products from the H + CH_4 → H_2 + CH_3 reaction. (b) Angular distributions of the CD_3 products from the H + CD_4 → H_2 + CD_3 reaction (ref 8). The distributions at different collisional energies for each reaction have been scaled according to the corresponding excitation function.

direction gradually, with nearly no contribution from the forward direction at all collision energies employed here. Classically, product scattering direction is closely related to the impact parameters in a direct reaction.[22] According to this simple picture, at collision energies just above the barrier (the classical barrier of the title reaction is 0.65 eV.[16]), only collisions with small impact parameters have enough energy to overcome the reaction barrier (including the centrifugal barrier) and lead to reactive scatterings, while collisions with larger impact parameters will not have enough energy to overcome

dx.doi.org/10.1021/jp501681h | J. Phys. Chem. A 2014, 118, 2426−2430

the reaction barrier due to the increased centrifugal barrier. The products are then backward scattered. Upon the increase of collision energy, collisions with larger impact parameters start to contribute, leading to smaller scattering angle (sideways and forward). Interestingly, for the reactions employed here, the contributions from the forward direction are negligible even at the collision energies much higher than the barrier.

The angular distributions of the CD_3 products from the H + CD_4 reaction[8] at the same collisional energies are also included in Figure 2b and show large similarities with those of the CH_3 products both in the general shape and the collisional energy dependence. However, the isotope effects are also very clear; at each collision energy, the CD_3 products are always scattered at more backward directions than the CH_3 products.

Similar behavior in the product angular distributions and their collisional energy dependence was observed previously in the Cl + CH_4 and Cl + CD_4 abstraction reactions, where a line-of-centers model incorporated with the shell concept was invoked to rationalize the main features.[23] The isotope effect on the product angular distribution in the Cl + CH_4/CD_4 reactions is more pronounced and was explained with the quantum tunneling and zero-point energy shift effects. For the H + CH_4/CD_4 reactions, these two quantum effects also point to the right direction; the higher zero-point energy for H + CH_4 would lead to a wider cone of acceptance, resulting into more sideways and forward scattered products. The tunneling effect also favors the H + CH_4 reaction, which would enhance the contributions of peripheral collisions, causing a more forward scattered distribution. These two quantum effects are expected to play important roles at collision energies close to the reaction barrier. However, the experimentally observed isotope effects are presented here even at the collision energy much higher than the reaction barrier, indicating that there might be another mechanism playing the dominant role. This will be further discussed in section 3.C, together with the isotope effects observed in the excitation function.

B. Product Kinetic Energy Distributions. The kinetic energy distributions of the CH_3 products are derived by integrating the corrected images along the scattering direction, which are then scaled to the total kinetic energy release spectra of the H_2 and CH_3 products based on the conservation of momentum, as shown in Figure 3a–d. From Figure 3, the collision energy dependence of vibrational and rotational excitations of the H_2 coproducts is clear. At the lowest collision energy (0.72 eV), there is only a single, slender peak, corresponding to the H_2 coproducts generated at the ground vibrational state with a cold rotational excitation. As the collision energy increases, higher vibrational states start to be populated; the rotational excitation also becomes hotter, causing a heavy overlap between different vibrational states. Nevertheless, for all collision energies studied here, the total translational energy distributions are all peaked close to the corresponding total available energy, indicating that most of the total available energy is partitioned as the translational energy of products.

The general shape of the product total kinetic energy release spectra of the H + CD_4 reaction and its collision energy dependence are similar to those of the H + CH_4 reaction. However, the difference in the internal state excitations of the HD/H_2 is also very clear; the rotational excitation of the HD is clearly colder than that of the H_2, especially at the lower collision energies, which makes the contributions from the H_2 at $\nu = 0$ and 1 partially resolved at the collision energy of 1.06 eV. The isotope effects are also clearly manifested in the vibrational state distributions of the H_2/HD products; similar to the H_2 products, the HD products are only populated at the ground vibrational state at the lowest collision energy (0.72 eV). However, with the increase of the collision energy, the vibrational excitation of HD increases more quickly. At the collision energy of 1.99 eV, the HD products are about one to two vibrational quanta hotter than the H_2 products produced at the same collision energy, and the total kinetic energy release spectra for these two reactions are clearly shifted from each other.

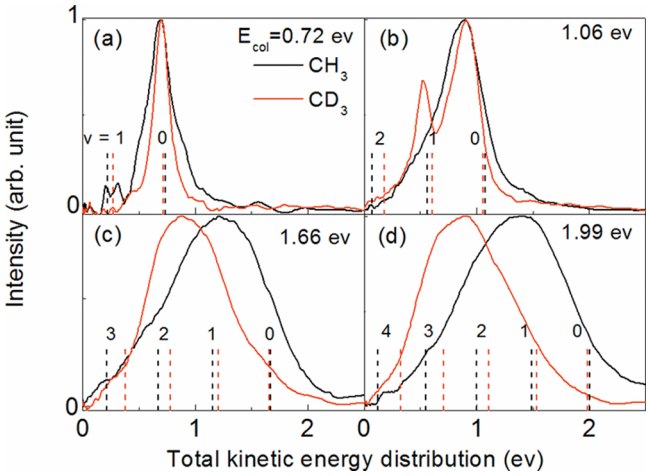

Figure 3. Total kinetic energy distributions of reaction products from H + CH_4 (black) and H + CD_4 (red) reactions at four different collision energies. The vertical dashed lines indicate the energetic limits for different vibrational states of the H_2 and HD coproducts. All of the distributions have been scaled to make the maxima equal to 1.

C. Excitation Function. The excitation function, which refers to the collision energy dependence of the ICS of a collision process, can be derived by integrating the corrected images along both the scattering angles and the radial directions and a careful calibration of the relative H beam intensities at four different velocities, as shown in Figure 4. We emphasize that only the excitation function for the ground vibrational state CH_3 channel is derived because only images of $CH_3(\nu = 0)$ were recorded in the current study due to the very small experimental signal. In a previous experimental study, CH_3 products with one quantum excitation of the umbrella mode were also observed.[20] However, it was found that the relative population of $CH_3(\nu = 0)$ and $CH_3(\nu_2 = 1)$ is largely independent of the collision energy in the range of 1.52–2.20 eV. Therefore, we take the measured excitation function for the $CH_3(\nu = 0)$ channel as a fair approximation of the excitation function for the entire abstraction reaction.

With the increase of collision energy, the ICS first increases, reaching a highest value, and then decreases. This collision energy dependence of ICS of the H + CH_4 reaction is very similar to that of the H + CD_4 reaction (also shown in Figure 4). However, the ICS increases much more slowly for the former reaction and reaches the maximum at a noticeably higher collision energy than the latter does. Due to the limited number of the collision energies studied experimentally, it is hard to extract the exact energetic position of the maximum of the excitation function. The experimental results for both reactions are in good agreement with the theoretical calculations,[8,16] which concluded that the ICS for the H +

dx.doi.org/10.1021/jp501681h | J. Phys. Chem. A 2014, 118, 2426–2430

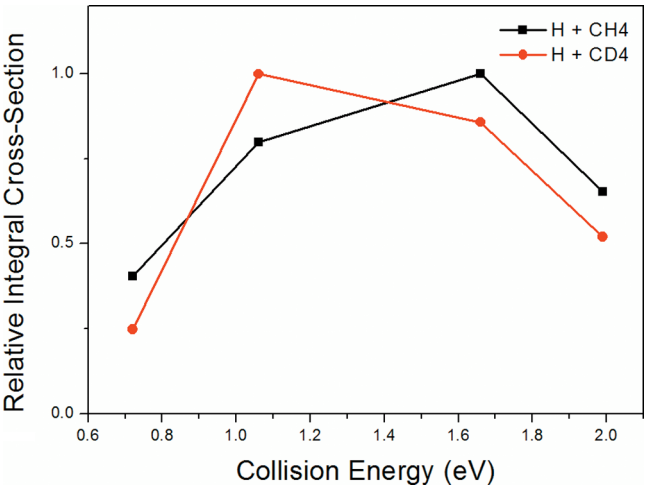

Figure 4. ISC (black) as a function of collision energy for the H + CH_4 → H_2 + $CH_3(\nu = 0)$ reaction, which represents a fair approximation of the excitation function of the total H + CH_4 abstraction reaction. The excitation function of the H + CD_4 → HD + CD_3 reaction (red) is also included for a direct comparison (ref 8). The intensities of the black and red curves have been normalized to unity at their maxima (see text and refs 8 and 16 for the (theoretical) relative intensities).

CD_4 reaction reaches the maximum at 1.2 eV, while for the H + CH_4 reaction, there is no sign of decrease of ICS until the collision energy is around 1.7 eV, suggesting that the maximum of the excitation function of the H + CH_4 reaction is at a collision energy about 0.5 eV higher than that of the H + CD_4 reaction. These theoretical calculations also concluded that the maximum ICS of the H + CH_4 reaction is more than twice as large as that of the H + CD_4 reaction.

In the above, the zero-point energy shift and tunneling effects were invoked to partly explain the observed isotope effects in the product angular distributions. However, it seems that neither of them can explain the observed isotope effects in the excitation function, considering that the reaction barrier difference between these two reactions due to the zero-point energy shift is less than 0.1 eV,[11] and the observed isotope effects happen at collision energies from the post-threshold region up to far above the reaction barrier.

The observed isotope effects are actually completely consistent with the mechanism proposed in our previous study on the H + CD_4 reaction; above the threshold, collisions with large impact parameters start to contribute, causing a rapid increase of the ICS. However, at collision energies far above the energy barrier, the incoming H atom moves too fast to be caught up by the slow D atom, causing a depression of reactivity.[8] The relative velocities of reactants in reactions of H + CH_4 and H + CD_4 are almost identical for the same collision energy. However, the H atom is twice as light as the D atom, which allows the H atom in CH_4 to follow the fast movement of the incoming H atom more easily, resulting in two effects: (1) The possibility for a peripheral collision leading to a reactive scattering becomes larger in the H + CH_4 reaction, which will cause more sideways/forward scattered product angular distributions, as observed in our experiments; (2) the ICS of the H + CH_4 reaction keeps increasing with the collision energy until at a noticeably higher collision energy than that of the H + CD_4 reaction; the maximum ICS of the H + CH_4 reaction is therefore expected to be larger than that of the H + CD_4 reaction. This expectation is consistent with the theoretical calculations in which the maximum ICS of the H + CH_4 reaction was found to be more than twice as large as that of the H + CD_4 reaction.[8,16] Therefore, the isotope effects observed here are in excellent agreement with the mechanism proposed in the previous study and further confirm it.

4. CONCLUSION

We have performed a detailed experimental study on the reaction dynamics of the H + CH_4 → H_2 + CH_3 reaction. The experimental results are compared extensively with those of the H + CD_4 → HD + CD_3 reaction, with emphasis on the isotope effects. The isotope effects are all observed in the product angular distributions, the product translational energy distributions, and the excitation function. These isotope effects are consistent with the reaction mechanism proposed previously in the H + CD_4 → HD + CD_3 reaction study and further confirm it.

AUTHOR INFORMATION

Corresponding Authors

*E-mail: wugr@dicp.ac.cn. Phone: +86-411-84379712 (G.W.).
*E-mail: xmyang@dicp.ac.cn. Phone: +86-411-84695174 (X.Y.).

Notes

The authors declare no competing financial interest.

ACKNOWLEDGMENTS

This work is supported by the National Natural Science Foundation of China, the Ministry of Science and Technology of China, and the Chinese Academy of Sciences.

REFERENCES

(1) Kurylo, M. J.; Hollinden, G. A.; Timmons, R. B. ESR Study of Kinetic Isotope Effect in Reaction of H and Deuterium Atoms with CH_4. *J. Chem. Phys.* **1970**, *52*, 1773−1781.
(2) Rabinowitz, M. J.; Sutherland, J. W.; Patterson, P. M.; Klemm, R. B. Direct Rate Constant Measurements for H + CH_4 → CH_3 + H_2, 897−1729 K, Using the Flash Photolysis-Shock Tube Technique. *J. Phys. Chem.* **1991**, *95*, 674−681.
(3) Germann, G. J.; Huh, Y. D.; Valentini, J. J. State-to-State Dynamics of Atom + Polyatom Abstraction Reactions. I. The H +CD_4→HD(V′,J′)+CD_3 Reaction. *J. Chem. Phys.* **1992**, *96*, 1957−1966.
(4) Camden, J. P.; Bechtel, H. A.; Zare, R. N. Dynamics of the Simplest Reaction of a Carbon Atom in a Tetrahedral Environment. *Angew. Chem., Int. Ed.* **2003**, *42*, 5227−5230.
(5) Camden, J. P.; Bechtel, H. A.; Brown, D. J. A.; Martin, M. R.; Zare, R. N.; Hu, W. F.; Lendvay, G.; Troya, D.; Schatz, G. C. A Reinterpretation of the Mechanism of the Simplest Reaction at an sp^3-Hybridized Carbon Atom: H + CD_4 → CD_3 + HD. *J. Am. Chem. Soc.* **2005**, *127*, 11898−11899.
(6) Camden, J. P.; Hu, W. F.; Bechtel, H. A.; Brown, D. J. A.; Martin, M. R.; Zare, R. N.; Lendvay, G.; Troya, D.; Schatz, G. C. H + CD_4 Abstraction Reaction Dynamics: Excitation Function and Angular Distributions. *J. Phys. Chem. A* **2006**, *110*, 677−686.
(7) Hu, W. F.; Lendvay, G.; Troya, D.; Schatz, G. C.; Camden, J. P.; Bechtel, H. A.; Brown, D. J. A.; Martin, M. R.; Zare, R. N. H + CD_4 Abstraction Reaction Dynamics: Product Energy Partitioning. *J. Phys. Chem. A* **2006**, *110*, 3017−3027.
(8) Zhang, W. Q.; Zhou, Y.; Wu, G. R.; Lu, Y. P.; Pan, H. L.; Fu, B. N.; Shuai, Q. A.; Liu, L.; Liu, S.; Zhang, L. L.; et al. Depression of Reactivity by the Collision Energy in the Single Barrier H + CD_4 → HD + CD_3 Reaction. *Proc. Natl. Acad. Sci. U.S.A.* **2010**, *107*, 12782−12785.

(9) Jordan, M. J. T.; Gilbert, R. G. Classical Trajectory Studies of the Reaction CH_4+H→CH_3+H_2. *J. Chem. Phys.* **1995**, *102*, 5669−5682.
(10) Espinosa-Garcia, J. New Analytical Potential Energy Surface for the CH_4+H Hydrogen Abstraction Reaction: Thermal Rate Constants and Kinetic Isotope Effects. *J. Chem. Phys.* **2002**, *116*, 10664−10673.
(11) Zhang, X.; Yang, G. H.; Han, K. L.; Wang, M. L.; Zhang, J. Z. H. Quantum Dynamics Study of Isotope Effect for H+CH_4 Reaction Using the SVRT Model. *J. Chem. Phys.* **2003**, *118*, 9266−9271.
(12) Wu, T.; Werner, H. J.; Manthe, U. First-Principles Theory for the H+CH_4 → H_2+CH_3 Reaction. *Science* **2004**, *306*, 2227−2229.
(13) Xie, Z.; Bowman, J. M.; Zhang, X. B. Quasiclassical Trajectory Study of the Reaction H+CH_4(ν_3=0,1)→CH_3+H_2 Using a New *Ab Initio* Potential Energy Surface. *J. Chem. Phys.* **2006**, *125*, 133120.
(14) Zhang, X. B.; Braams, B. J.; Bowman, J. M. An *Ab Initio* Potential Surface Describing Abstraction and Exchange for H+CH_4. *J. Chem. Phys.* **2006**, *124*, 021104.
(15) Albu, T. V.; Espinosa-Garcia, J.; Truhlar, D. G. Computational Chemistry of Polyatomic Reaction Kinetics and Dynamics: The Quest for an Accurate CH_5 Potential Energy Surface. *Chem. Rev.* **2007**, *107*, 5101−5132.
(16) Zhou, Y.; Fu, B. N.; Wang, C. R.; Collins, M. A.; Zhang, D. H. *Ab Initio* Potential Energy Surface and Quantum Dynamics for the H + CH_4 → H_2 + CH_3 Reaction. *J. Chem. Phys.* **2011**, *134*, 064323.
(17) Wu, G.; Zhang, W.; Pan, H.; Shuai, Q.; Jiang, B.; Dai, D.; Yang, X. A New Crossed Molecular Beam Apparatus Using Time-Sliced Ion Velocity Imaging Technique. *Rev. Sci. Instrum.* **2008**, *79*, 094104.
(18) Langford, S. R.; Regan, P. M.; Orr-Ewing, A. J.; Ashfold, M. N. R. On the UV Photodissociation Dynamics of Hydrogen Iodide. *Chem. Phys.* **1998**, *231*, 245−260.
(19) Hudgens, J. W.; DiGiuseppe, T. G.; Lin, M. C. Two Photon Resonance Enhanced Multiphoton Ionization Spectroscopy and State Assignments of the Methyl Radical. *J. Chem. Phys.* **1983**, *79*, 571−582.
(20) Camden, J. P.; Bechtel, H. A.; Brown, D. J. A.; Zare, R. N. Effects of C-H Stretch Excitation on the H+CH_4 Reaction. *J. Chem. Phys.* **2005**, *123*, 134301.
(21) Lin, J. J.; Zhou, J.; Shiu, W.; Liu, K. Application of Time-Sliced Ion Velocity Imaging to Crossed Molecular Beam Experiments. *Rev. Sci. Instrum.* **2003**, *74*, 2495−2500.
(22) Levine, R. D. *Molecular Reaction Dynamics*; Cambridge University Press: Cambridge, U.K., 2005.
(23) Zhang, B.; Liu, K. Imaging a Reactive Resonance in the Cl + CH_4 Reaction. *J. Chem. Phys.* **2005**, *122*, 101102−101102.